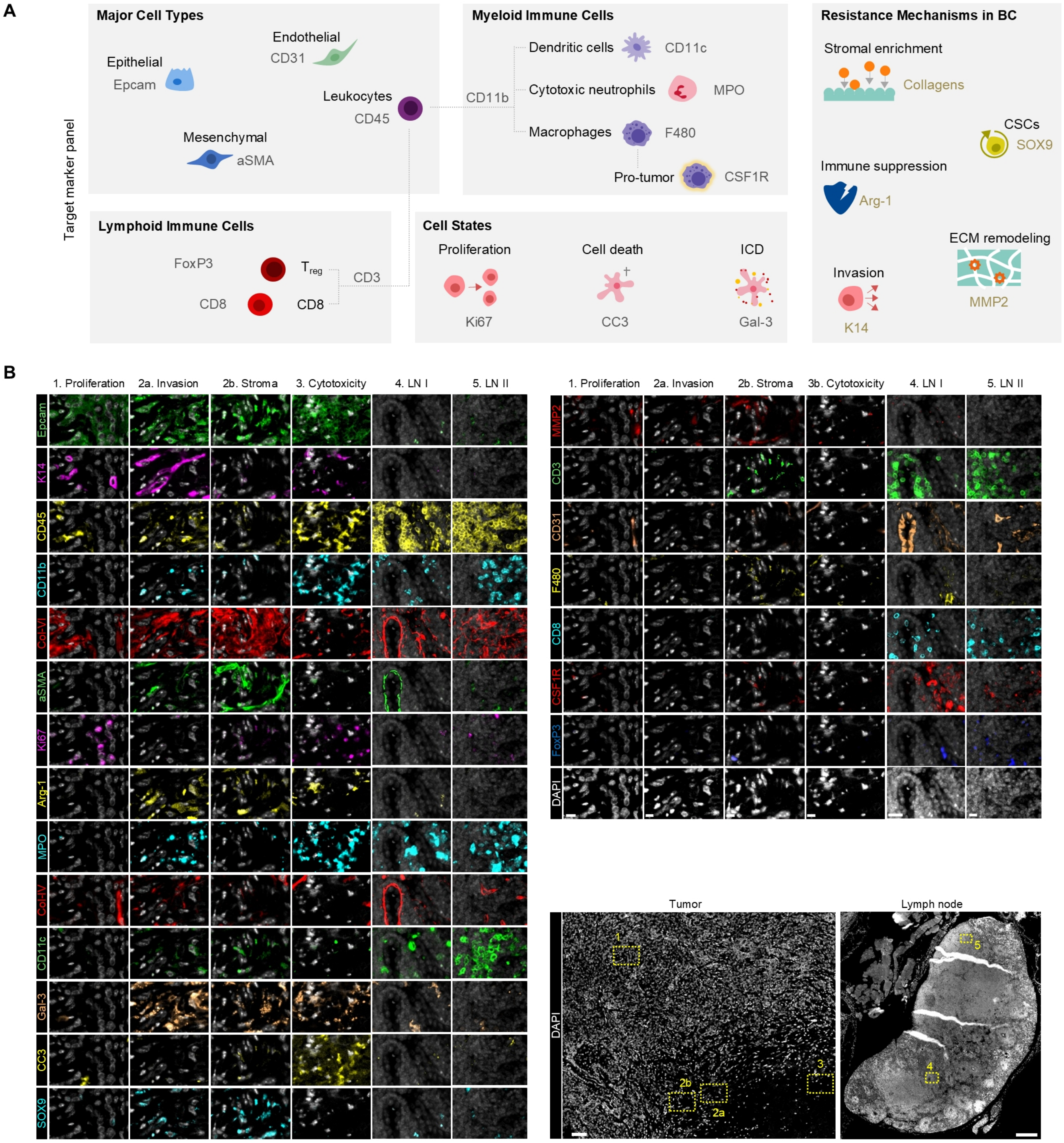

Supplementary Figure 1 | Target marker panel and expression in MMTV-PyMT. A, Protein targets of the cyclic immunofluorescence marker panel include key cell types, immune cell subclassification, breast cancer resistance mechanisms and response/cell status antibodies. **B,** Representative phenotype images of each marker in three regions from the panobinostat ROI (1.-3.) and comparison to lymph node phenotypes (4., 5.) For target marker expression in whole panobinostat vs control ROI and whole lymph node see Extended Data Image sequences. Scale bars: 5 µm (1.-3.), 10 µm (4., 5.), 50 µm (tumor), 200 µm (LN).

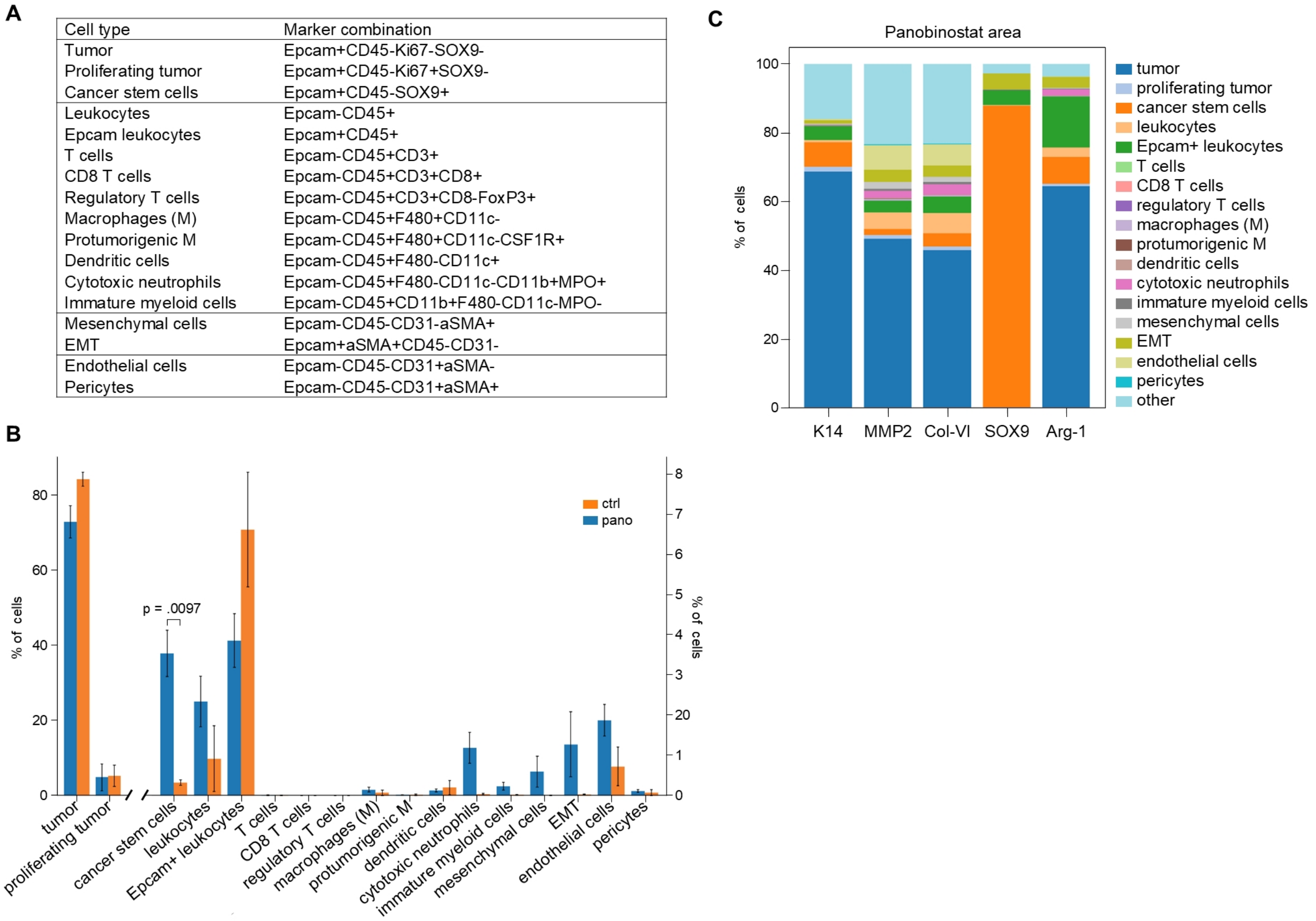

Cell type	Marker combination
Tumor	Epcam+CD45-Ki67-SOX9-
Proliferating tumor	Epcam+CD45-Ki67+SOX9-
Cancer stem cells	Epcam+CD45-SOX9+
Leukocytes	Epcam-CD45+
Epcam leukocytes	Epcam+CD45+
T cells	Epcam-CD45+CD3+
CD8 T cells	Epcam-CD45+CD3+CD8+
Regulatory T cells	Epcam-CD45+CD3+CD8-FoxP3+
Macrophages (M)	Epcam-CD45+F480+CD11c-
Protumorigenic M	Epcam-CD45+F480+CD11c-CSF1R+
Dendritic cells	Epcam-CD45+F480-CD11c+
Cytotoxic neutrophils	Epcam-CD45+F480-CD11c-CD11b+MPO+
Immature myeloid cells	Epcam-CD45+CD11b+F480-CD11c-MPO-
Mesenchymal cells	Epcam-CD45-CD31-aSMA+
EMT	Epcam+aSMA+CD45-CD31-
Endothelial cells	Epcam-CD45-CD31+aSMA-
Pericytes	Epcam-CD45-CD31+aSMA+

Supplementary Figure 2 | Hierarchical gating and biology-based quantification of cell types. A, Hierarchical gating strategy and marker combinations for standard cell type quantification. **B,** Mean standard cell type abundance in n=4 replicates upon local treatment compared to tumor bed using gating strategy from (A) presented as mean ± standard error of mean. Statistical significance calculated using paired sample students t test. **C,** Mean standard cell type quantification of resistance marker-positive cells in the panobinostat assay area from n=4 replicates, using gating strategy from (a).

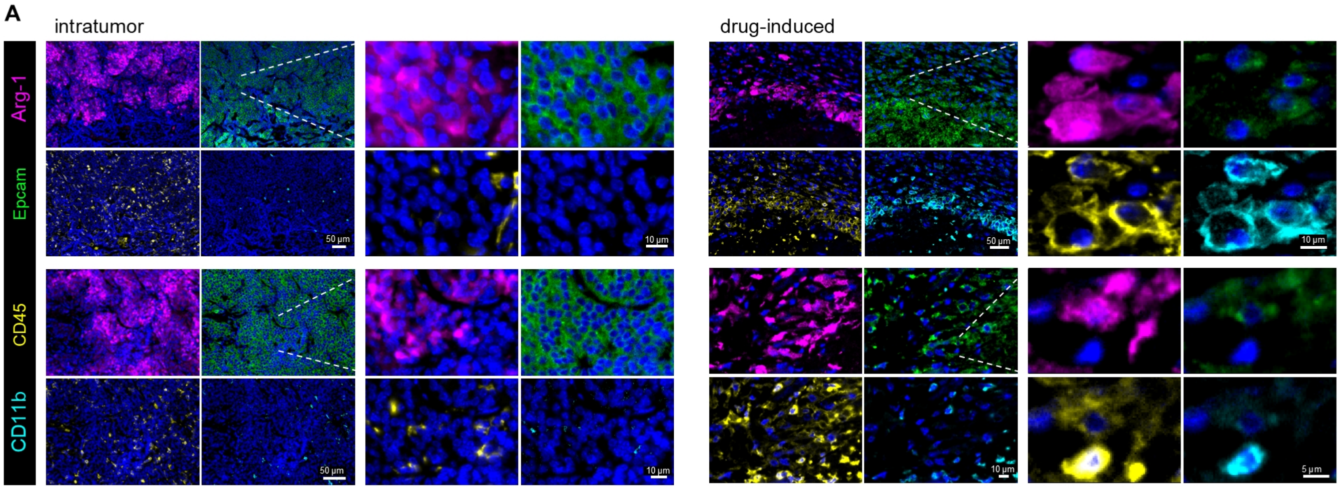

Supplementary Figure 3 | Location-based differential expression of Arg-1. A, Representative images of Arg-1 expression on Epcam+ tumor cells in the tumor bed (left) vs Arg-1 expression on myeloid cells in the drug-affected assay area (right, drug-induced).

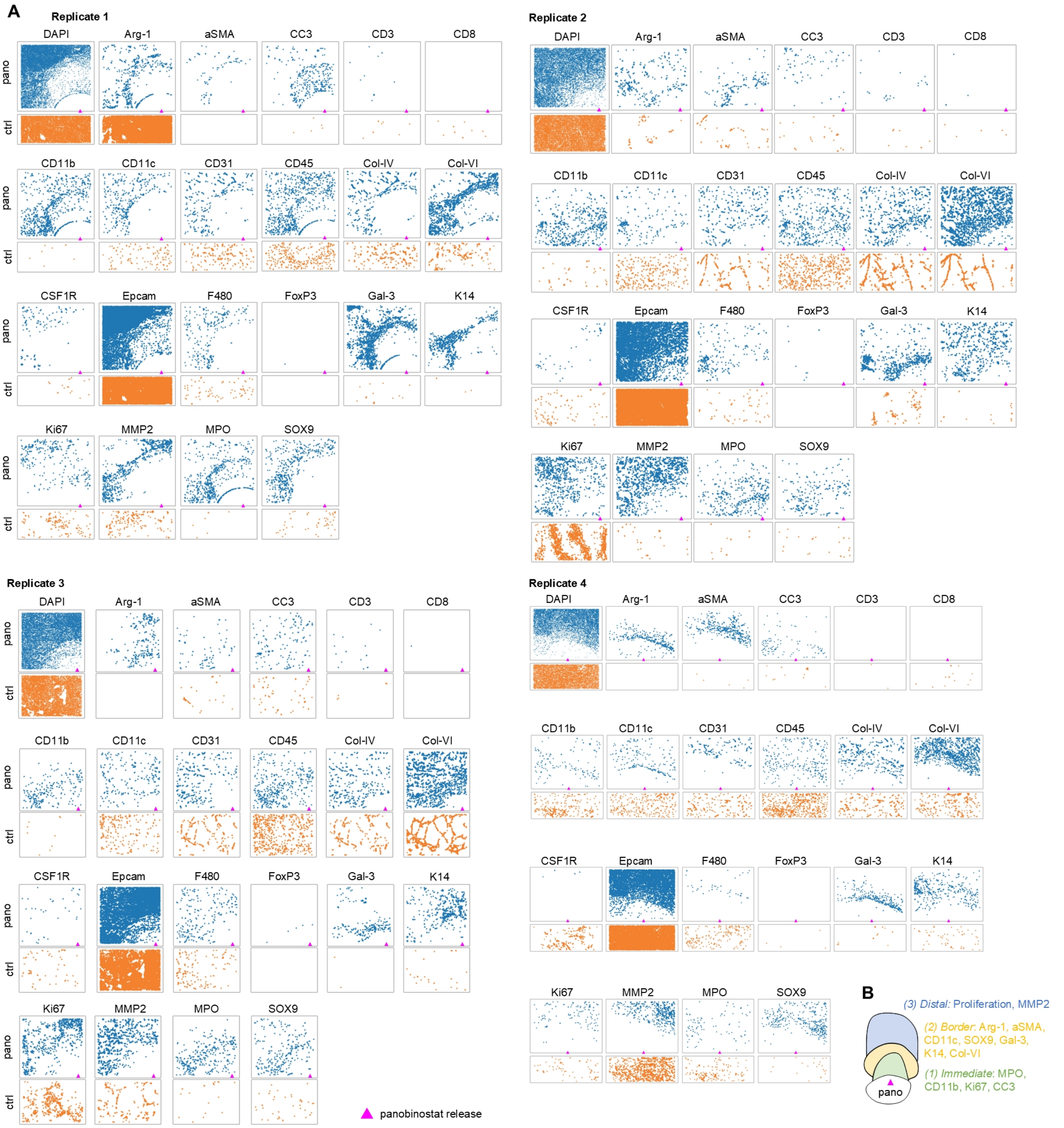

Supplementary Figure 4 | Spatial target marker expression in layers. A, Single-cell marker expression in xy space. Positive single-cell events for all individual markers per replicate, dots equal marker-positive cell. **B,** Schematic representation of cell phenotype separation into zones with distance from the panobinostat well. MPO+ cytotoxic neutrophils are recruited into *immediate* proximity and this phenotype is halt by the *border* barrier composed of aSMA mesenchymal cells, CD11c dendritic cells, SOX9 cancer stem cells, Galectin-3, Arg-1 immune suppressive cells, K14 cells of invasive front and ECM deposition (Col-VI), the last two propagating into the *distal* zone. Proliferation and matrix remodeling (MMP2) are dominant markers in the *distal* zone.

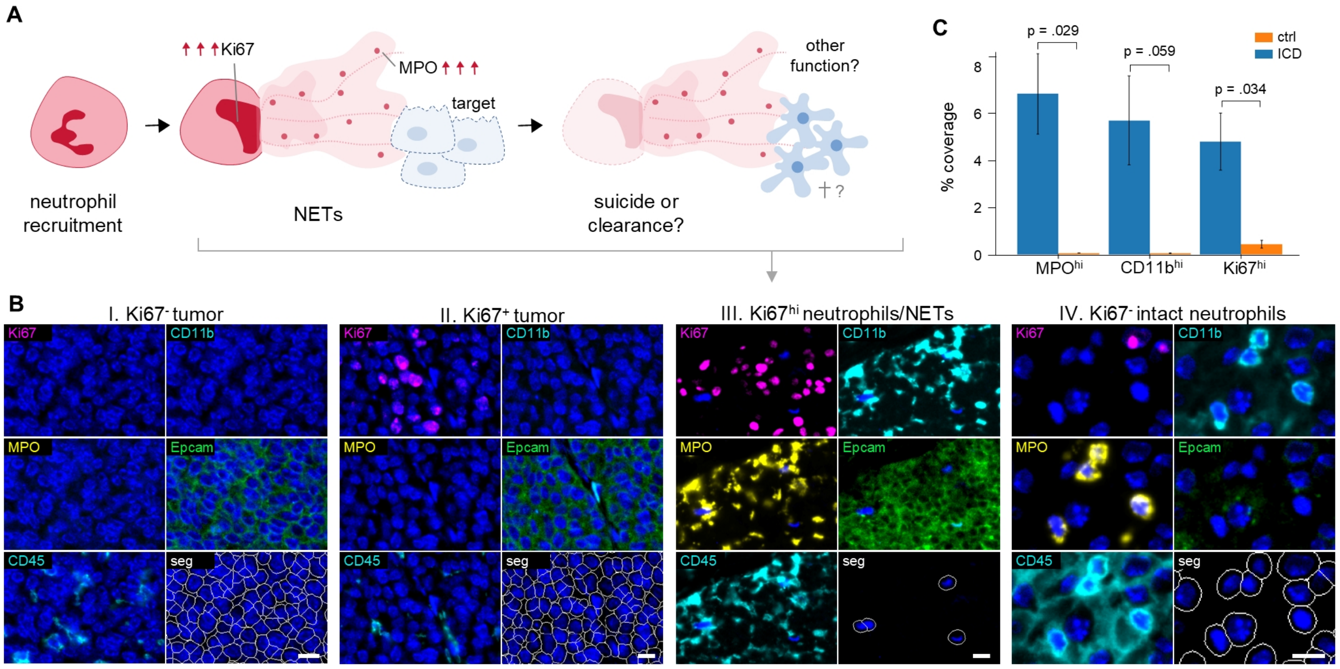

Supplementary Figure 5 | Neutrophil extracellular trap (NET) formation with prolonged panobinostat exposure. A, Schematics depicting NET formation. **B,** Representative images of Ki67$^-$ tumor, Ki67$^+$ tumor, Ki67^{hi} neutrophils/NETs and Ki67$^-$ intact neutrophils using the same thresholds for each marker. White outlines (seg) and DAPI (blue) illustrate lack of segmentation of NETs in III. Scale bars: 10 µm. **C,** Quantification of marker coverage (pixel value) of CD11b-positive and Ki67 and MPO-high signal in the representative cell death regions in the assay area vs intratumor control. The graph shows mean ± s.e.m.; n = 4 wells and significance was calculated using paired sample students t-test. ICD: immunogenic cell death.

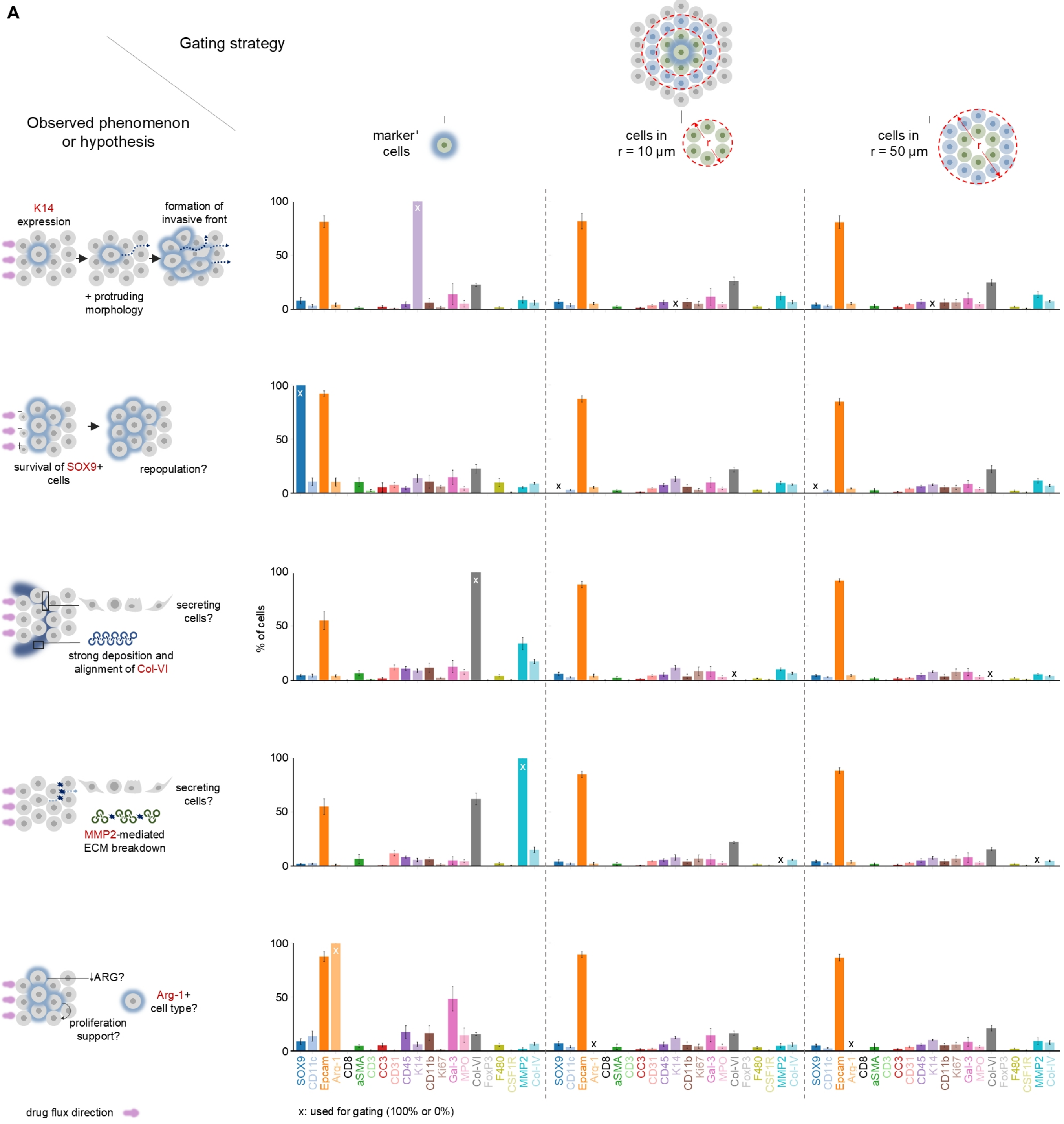

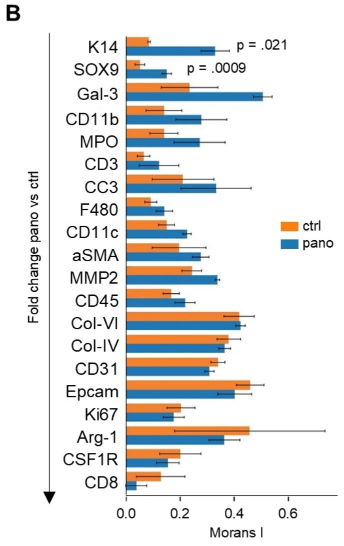

Supplementary Figure 6 | Quantification of resistance biomarker events of positive cells, their immediate surrounding architecture and spatial variability. A, Resistance marker positive cells and their surrounding marker expression. Left panel: Observed phenomena and hypothesis in the assay area induced by the panobinostat release. Center to right panels: Quantification of biomarkers on resistance marker positive cells, and quantification of biomarkers on cells in immediate and intermediate proximity (10, 50 µm radius, respectively) to resistance marker-positive cells. Total cell number given in graph itself, from n=4 replicates from two tumors. **"x"** in graphs denotes the marker used for gating. **B,** Absolut Morans I values from n = 4 replicates presented as mean ± standard error of mean. Fold change between panobinostat area versus control intratumor presented in Fig. 2b. Significance was calculated using paired students t-test. FoxP3 marker was excluded due to scarce expression not allowing meaningful analysis.

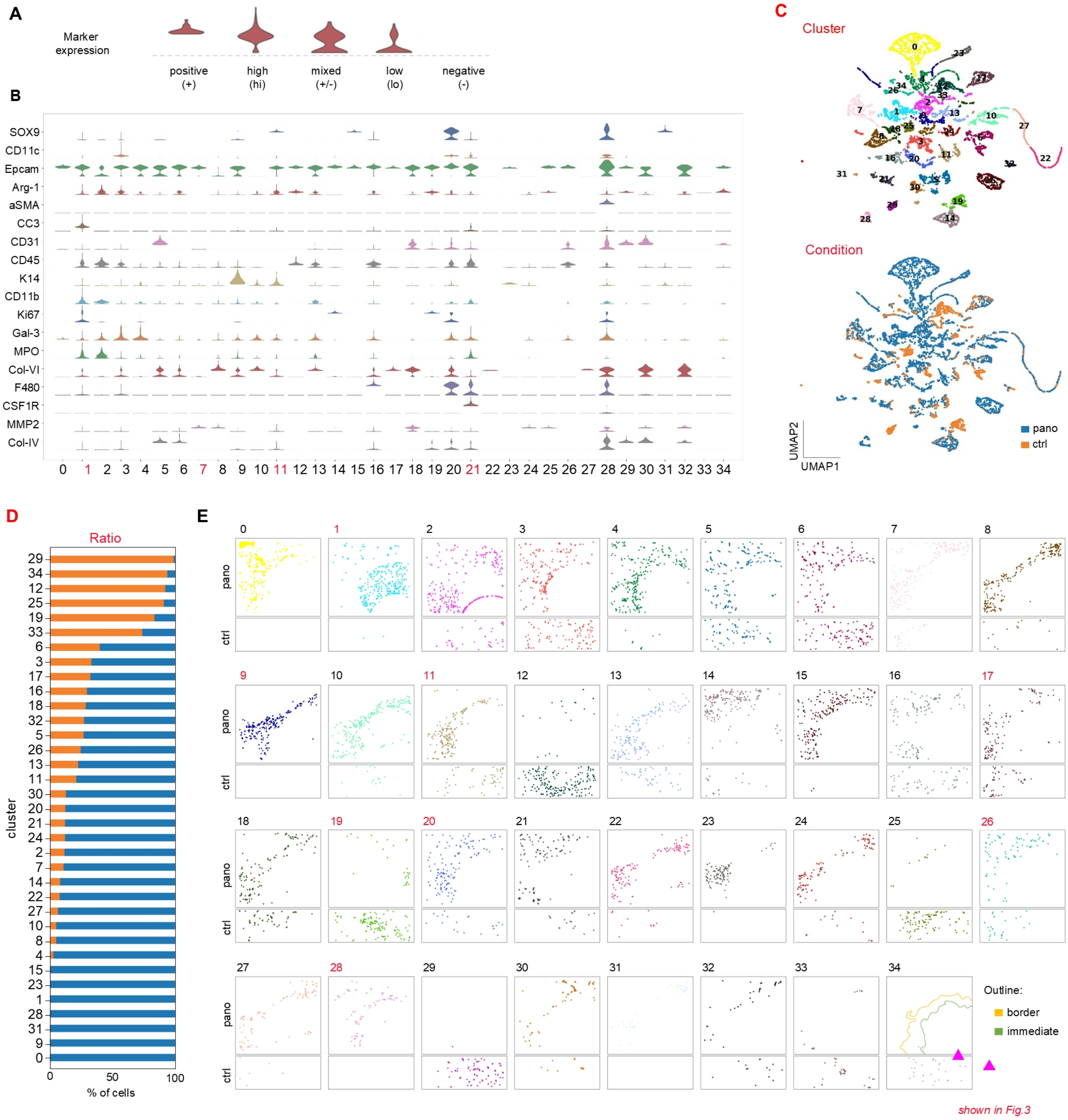

Supplementary Figure 7 | Differential unsupervised clustering facilitated discovery of multi-marker combinations in replicate 1. A, Annotation strategy for violin plots**. B,** Violin plot denoting marker expression in each cluster from unsupervised cluster analysis, for full annotation see Extended Data Table 2. **C,** UMAP representation colored by cluster (top) or condition (bottom). **D,** Cluster ratios between conditions for each cluster. **E,** Spatial representation of each cluster, top graph shows distribution in experimental area, bottom shows intratumor control. Parts of this figure are shown in Main Fig. 3, essential parts are highlighted in red.

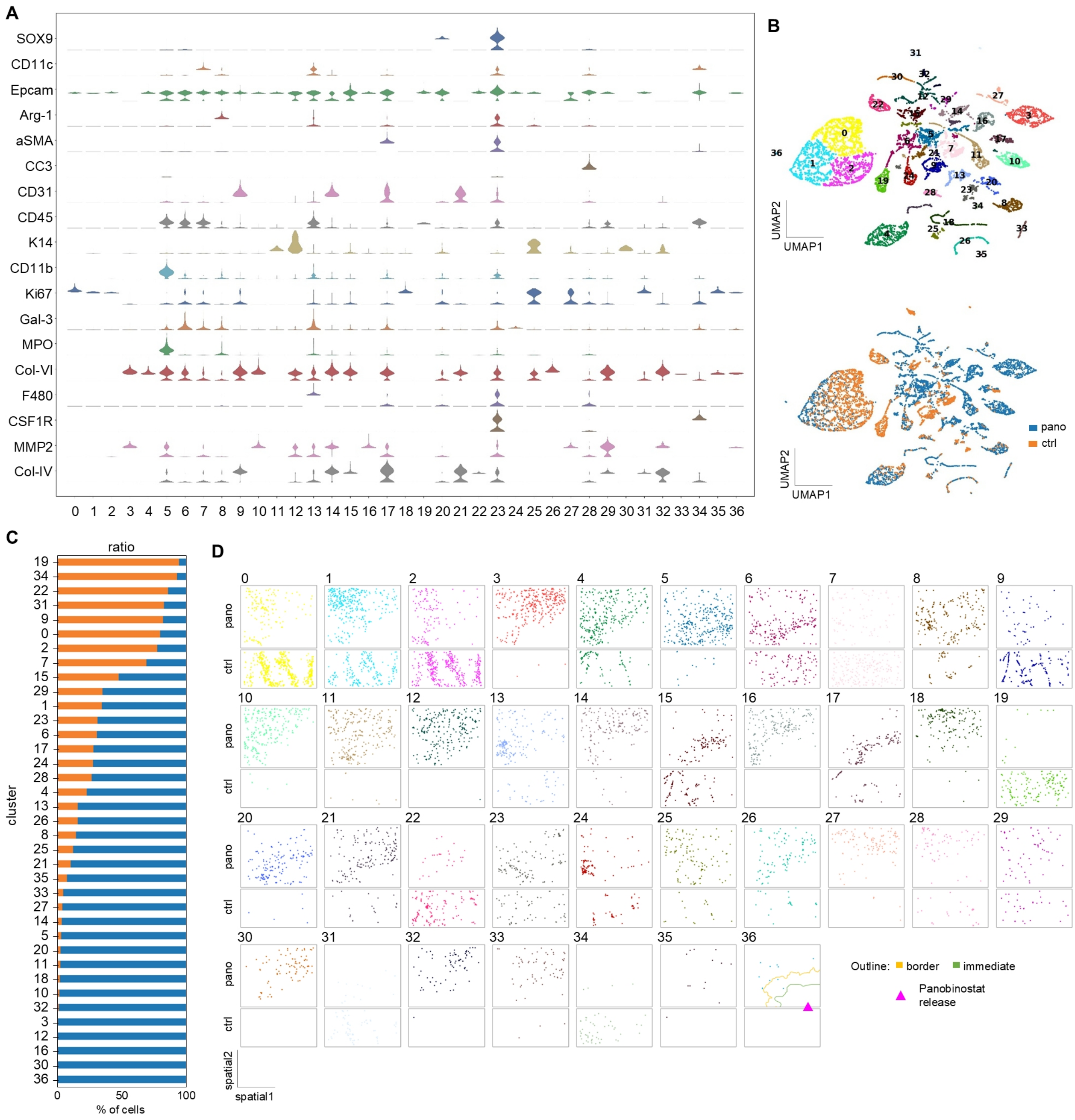

Supplementary Figure 8 | Differential unsupervised clustering facilitated discovery of multi-marker combinations in replicate 2. A, Violin plot denoting marker expression in each cluster from unsupervised cluster analysis, for full annotation see Extended Data Table 2. **B,** UMAP representation colored by cluster (top) or condition (bottom). **C,** Cluster ratios between conditions for each cluster. **D,** Spatial representation of each cluster, top graph shows distribution in experimental area, bottom shows intratumor control.

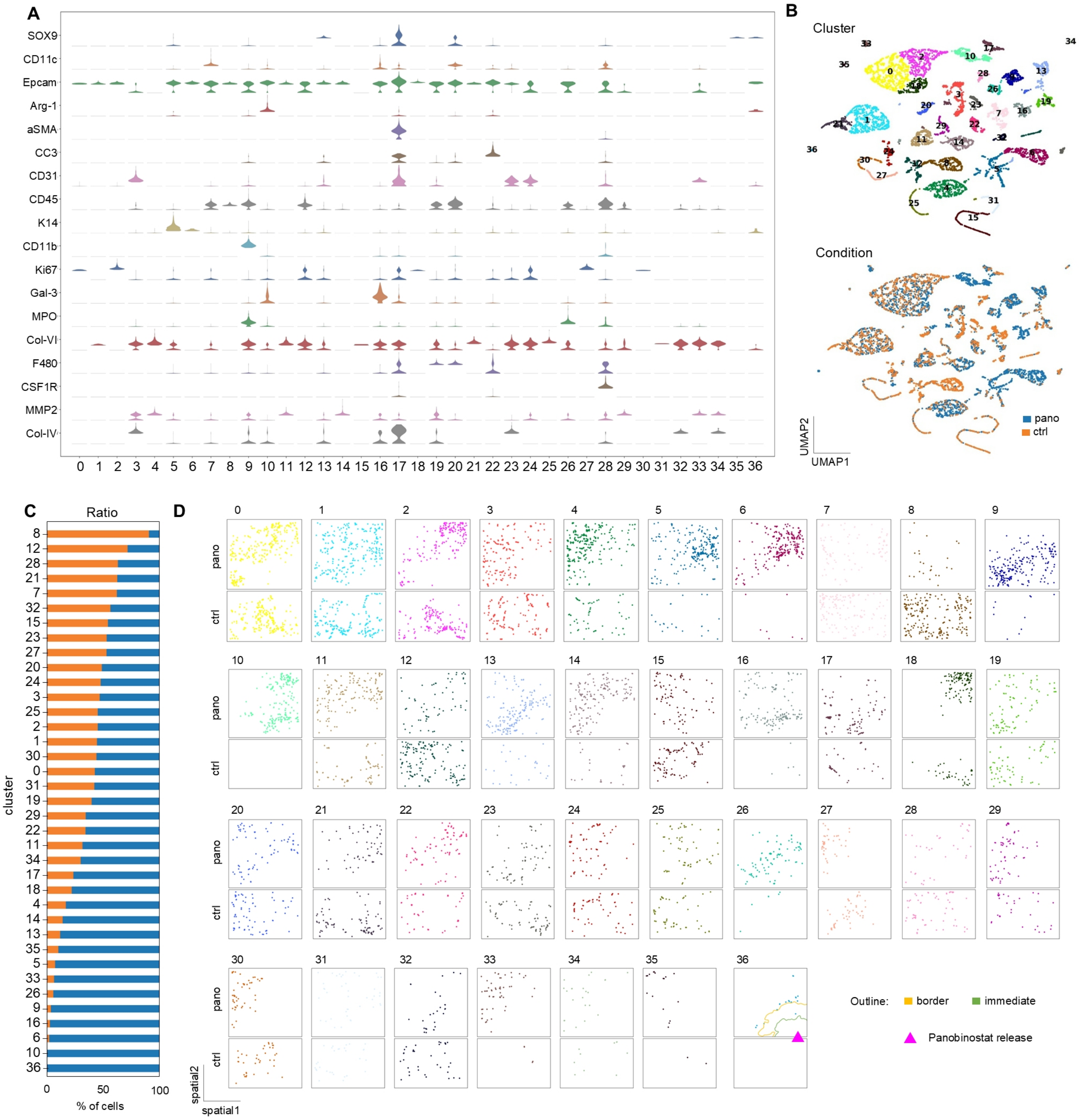

Supplementary Figure 8 | Differential unsupervised clustering facilitated discovery of multi-marker combinations in replicate 3. A, Violin plot denoting marker expression in each cluster from unsupervised cluster analysis, for full annotation see Extended Data Table 2. **B,** UMAP representation colored by cluster (top) or condition (bottom). **C,** Cluster ratios between conditions for each cluster. **D,** Spatial representation of each cluster, top graph shows distribution in experimental area, bottom shows intratumor control.

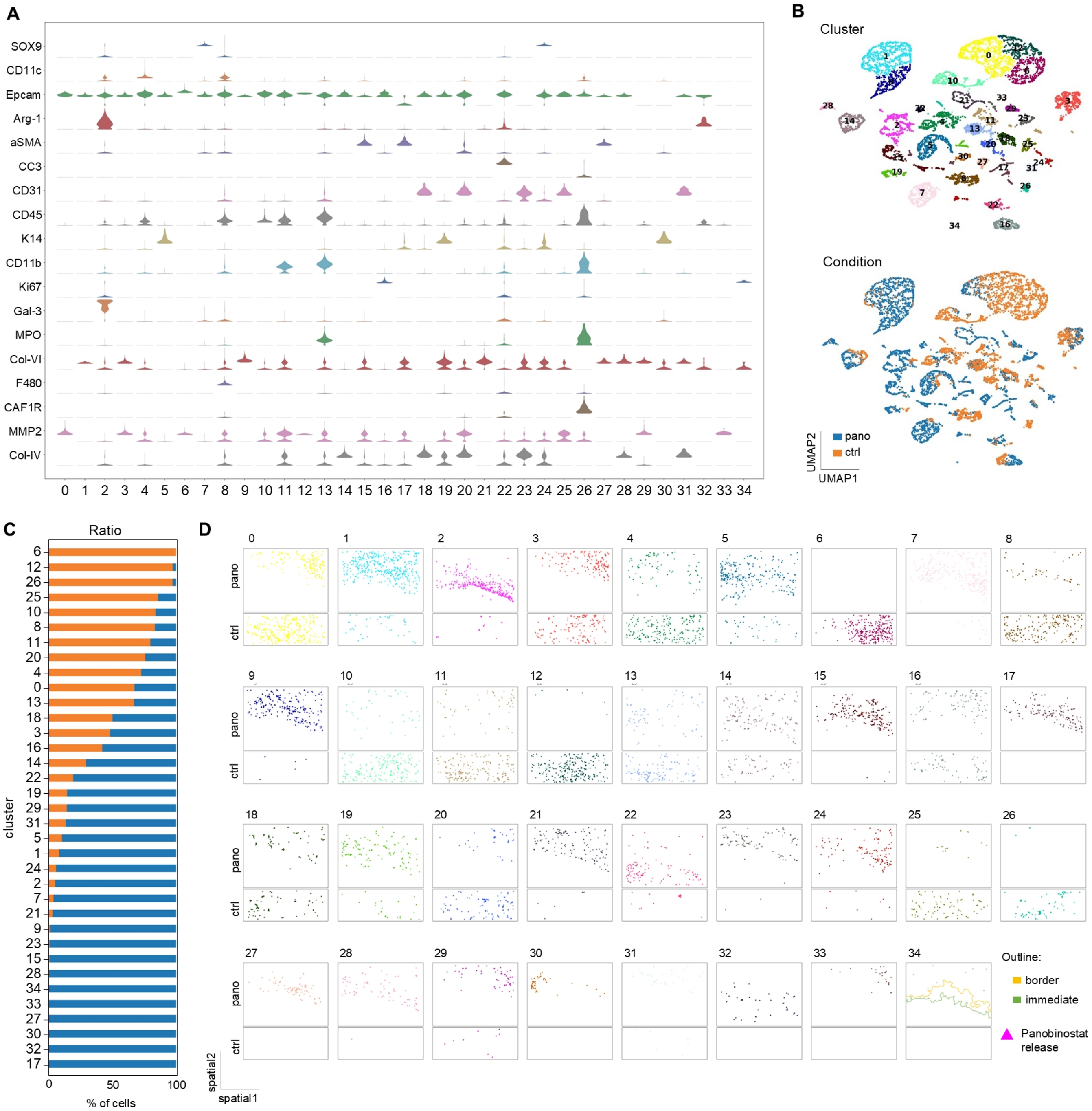

Supplementary Figure 10 | Differential unsupervised clustering facilitated discovery of multi-marker combinations in replicate 4. A, Violin plot denoting marker expression in each cluster from unsupervised cluster analysis, for full annotation see Extended Data Table 3. **B,** UMAP representation colored by cluster (top) or condition (bottom). **C,** Cluster ratios between conditions for each cluster. **D,** Spatial representation of each cluster, top graph shows distribution in experimental area, bottom shows intratumor control.

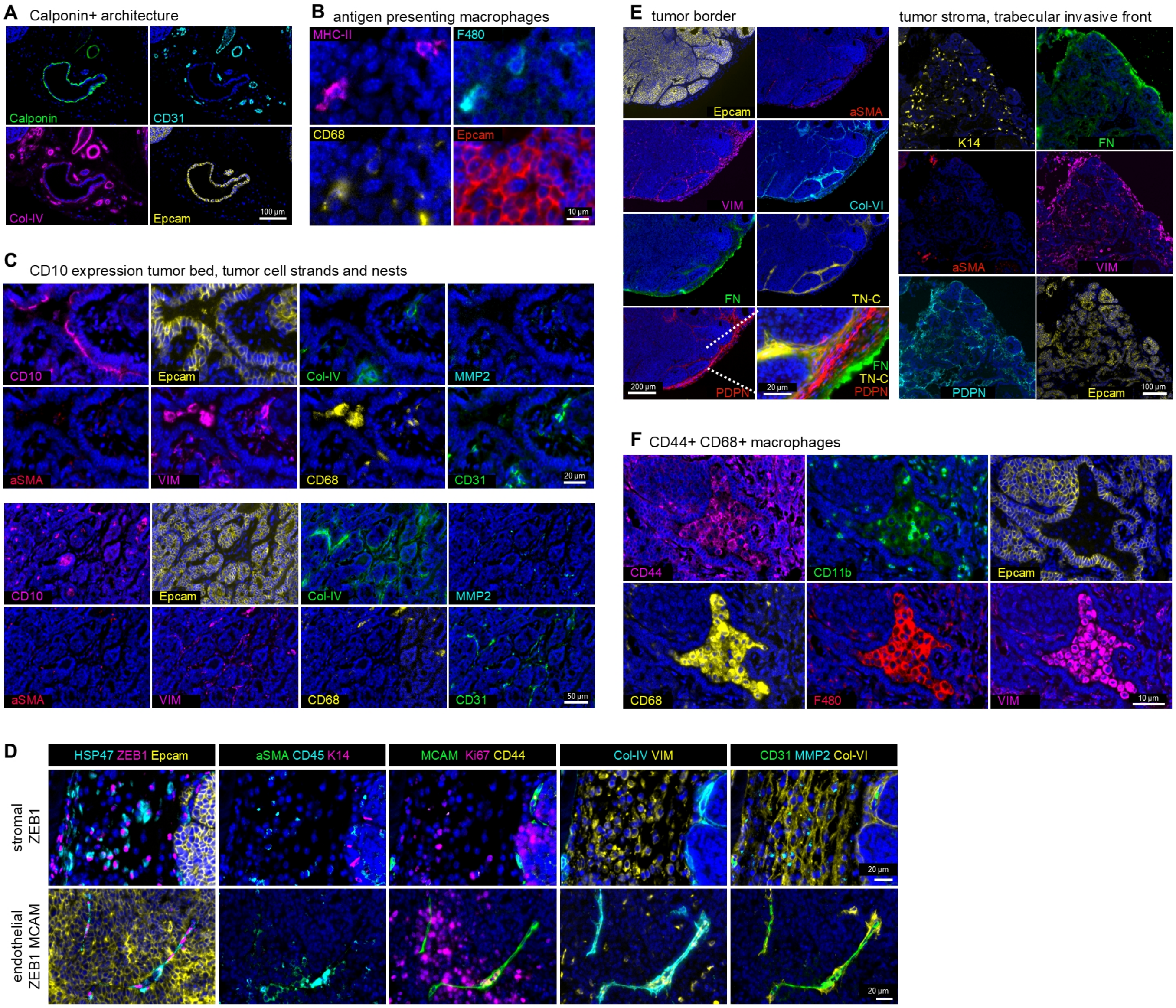

Supplementary Figure 11 | Extended panel for fibroblast subclassification representative staining of cyclic immunofluorescence. A, Rare myoepithelial/contractile calponin architecture in peritumor. **B,** MHC-II positive antigen-presenting macrophages in the tumor bed. **C,** Polarized CD10 expression by aligned tumor cells (top) or inside the intercellular space of tumor nests (bottom). **D,** ZEB1 expression in stromal cells of round shape (top) and endothelial expression of ZEB1 and MCAM in the tumor bed (bottom). **E,** Respective fibroblast marker staining illustrating different subsets of fibroblasts and populations with shared expression. Tumor margins at the outmost periphery show highest Fibronectin expression levels. **F,** CD44+ CD68+ macrophage aggregate inside the tumor bed. Expression of cytoskeletal VIM protein and CD44 might indicate cell migration capacities. Scale bars as indicated in the images.

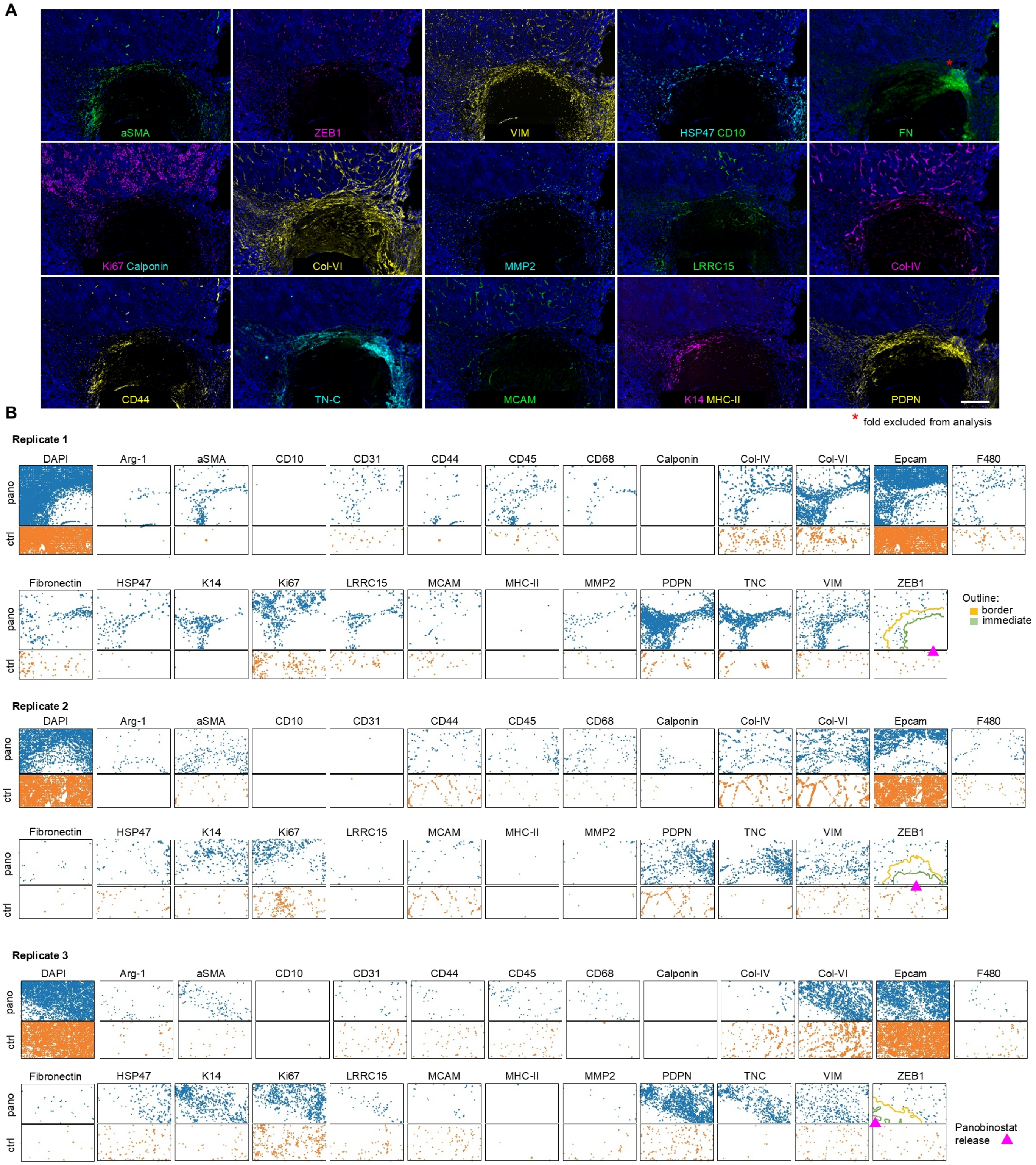

Supplementary Figure 12 | Distribution of extended panel markers in MMTV-PyMT panobinostat treated region. A, Representative staining images of a representative tissue section surrounding the implantable microdevice containing panobinostat for eight days stained with cycIF, panel of antibodies listed in Fig. 4a. Scale bar: 200 µm. **B,** Representative DNA (DAPI nuclear stain, total cells) and selected target marker expression in xy-space, dots equal marker-positive cells in three replicates. Magenta triangle indicates drug release upwards.

Supplementary Figure 13 | Unsupervised clustering of the extended panel fibroblast data set. A-C, UMAP representations of clustering of 14800 cells merged from three replicates colored by cluster (A.), condition (B.) and replicate (C.). Clustering parameters were n_neighbors= 100, resolution = 0.075 and were chosen to get a broad overview over the data to select the fibroblast and macrophage clusters of interest. **D,** Marker expression (depicted as violin plots) for unsupervised clusters. Cluster 1 and 9 were selected for subclustering (Fig. 4, Fig. 1S4). **E,** Spatial representation of clusters in three replicates. Top and bottom graph illustrate distribution in panobinostat-affected and random intratumor control, respectively.

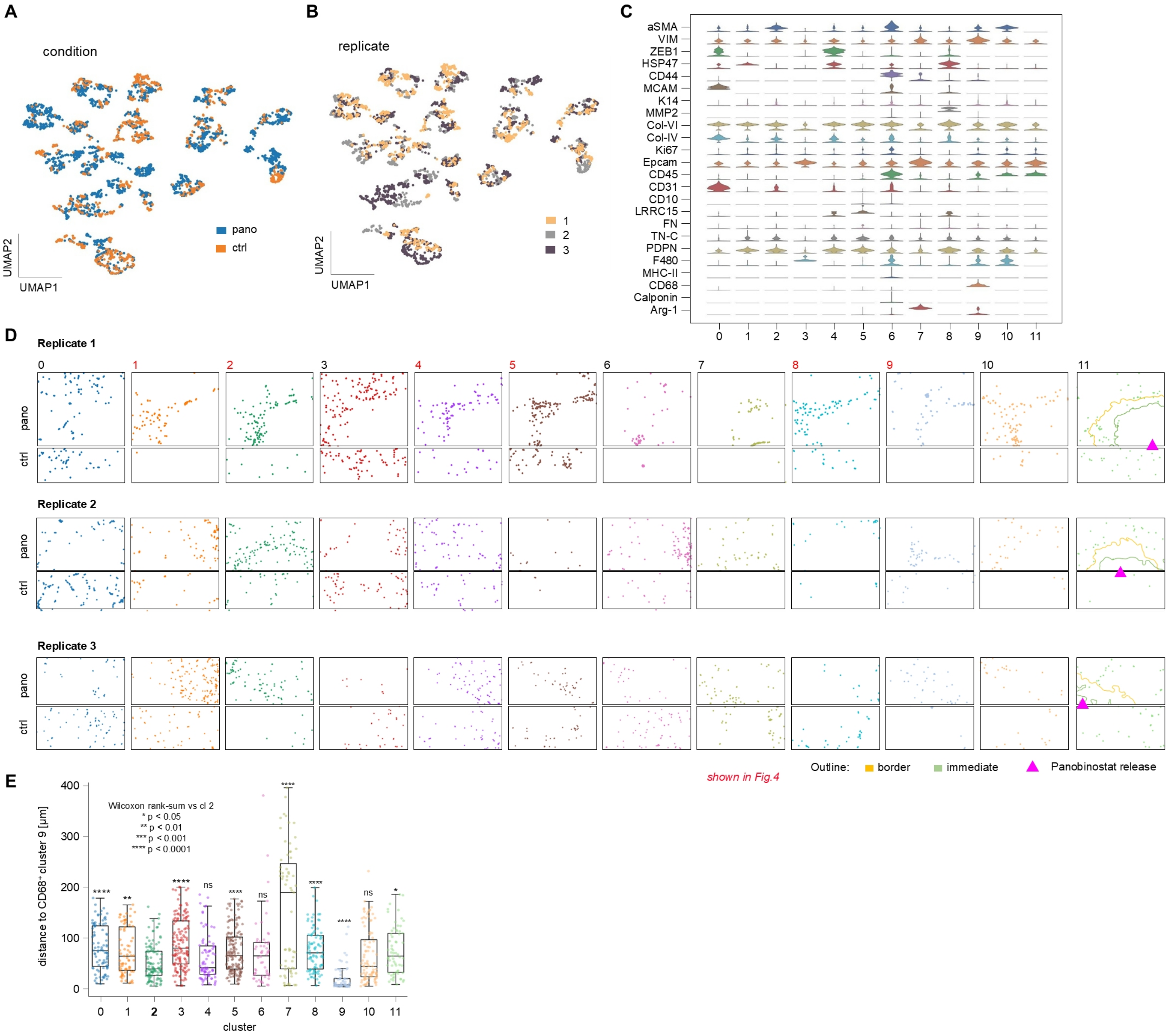

Supplementary Figure 14 | Unsupervised subclustering of the fibroblast-associated clusters. A-B, UMAP representations of clustering of 3488 cells merged from three replicates colored by condition (A.) and replicate (B.). Clustering parameters were n_neighbors= 15, resolution = 0.05 and were chosen to get a broad overview over the data to select the fibroblast and macrophage clusters of interest. **C,** Marker expression (depicted as violin plots) for unsupervised clusters. **D,** Spatial representation of clusters in three replicates. Top and bottom graph illustrate distribution in panobinostat-affected and random intratumor control, respectively. **E.** Boxplots showing distance quantification of each cell per cluster to the closest CD68+ macrophage (of cluster 9) in replicate 1. The box shows the median and the quartiles of the distribution, whiskers correspond to 1.5 interquartile range of the lower and upper quartile; outliers are exempt. Pairwise comparisons against cluster 2 distribution were determined using a two-sided Wilcoxon rank-sum test. Parts of this figure are shown in Main Fig. 4, essentials are highlighted in red.

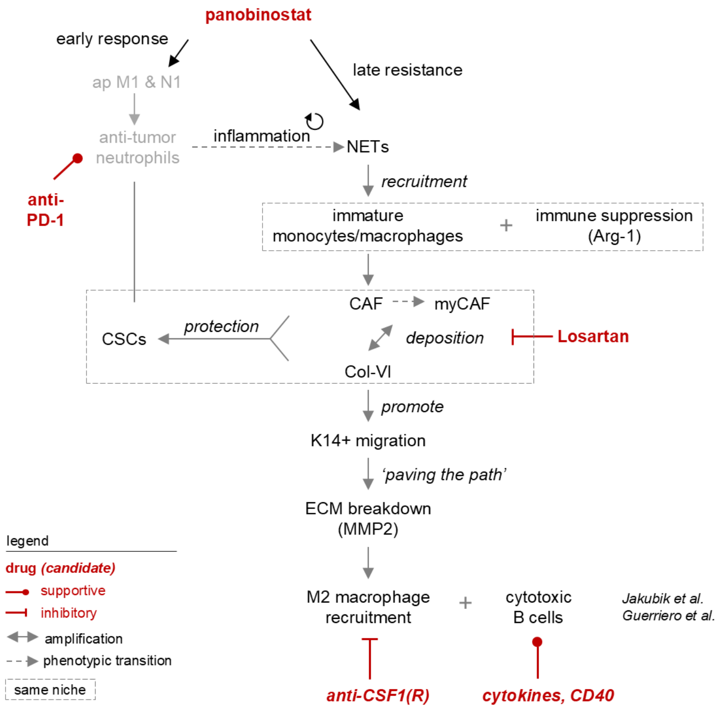

Supplementary Figure 15 | Flow diagram depicting hypothesized sequence of events induced by prolonged panobinostat stimulus. Line flow diagram of a proposed panobinostat mechanism of action at a late timepoint determined by MIMA in this study and targetable axis with proposed drug candidate. Phenotypes in grey color (early response mechanisms) have been derived from three-day implant studies conducted previously and tested successfully in vivo (Tatarova at al, 2022; Jakubik et al., under review). Other phenotypes derived from eight-day implantation in this study. Targeting the macrophage axis and B cells (*italic*) have been identified and tested (macrophages only) in the literature (Guerriero et al, 2017; Jakubik et al.,under review) but not as part of this study. Legend in figure itself.

Target	Clone	Origin	Vendor
SOX9	D8G8H	Rabbit	Cell Signaling Technology
CD11c	D1V9Y	Rabbit	Cell Signaling Technology
Epcam	R002	Rabbit	Sino Biological
Arg-1	D4E3M	Rabbit	Cell Signaling Technology
CD8	4S145	Rabbit	Invitrogen
aSMA	D4K9N	Rabbit	Cell Signaling Technology
CD3	D4V8L	Rabbit	Cell Signaling Technology
CC3 Asp175	D3E9	Rabbit	Cell Signaling Technology
CD31	EPR17260	Rabbit	Abcam
CD31	D8V9E	Rabbit	Cell Signaling Technology
CD45		Rabbit	
CD45	D3F8Q	Rabbit	Cell Signaling Technology
K14	EPR17350	Rabbit	Abcam
CD11b		Rabbit	Abcam
Ki67	D3B5	Rabbit	Cell Signaling Technology
FoxP3	polyclonal	Rabbit	Novus Biologicals
Gal-3	M3/38	Rat	Biolegend
MPO	polyclonal	Goat	R&D systems
Col-VI	EPR17072	Rabbit	Abcam
F480	D2S9R	Rabbit	Cell Signaling Technology
CSF1R	Polyclonal	Rabbit	Sino Biological
MMP2	EPR1184	Rabbit	Abcam
Col-IV	Polyclonal	Rabbit	MD Biosciences
MHC-II	M5/114.15.2	Rat	Biolegend
CD44	E7K2Y	Rabbit	Cell Signaling Technology
CD10	F4P6H	Rabbit	Cell Signaling Technology
ZEB1	E2G6Y	Rabbit	Cell Signaling Technology
VIM	D21H3	Rabbit	Cell Signaling Technology
HSP47	EPR4217	Rabbit	Abcam
TN-C	EPR4219	Rabbit	Abcam
FN	F14	Rabbit	Abcam
Calponin	D8L2T	Rabbit	Cell Signaling Technology
LRRC15	E4X8J	Rabbit	Cell Signaling Technology
PDPN	8.1.1	Hamster	Novus Biologicals
MCAM	E3F3E	Rabbit	Cell Signaling Technology
CD68	E3O7V	Rabbit	Cell Signaling Technology

Supplementary Table 1 I Cyclic immunofluorescence antibodies.

Replicate 1		Ratio		
Cluster	Marker combination	ctrl	pano	Phenotype
0	Epcam^{+}Gal-3^{+}	0	538	Gal-3+ tumor
1	Epcam^{+}CC3^{+}CD45$^{+/-}$CD11b^{hi}MPO^{hi}Ki67^{lo}Col-VI^{lo}	2	379	Dying tumor (+cytotoxic neutrophils)
2	CD45^{hi}CD11b^{hi}MPO^{+}Epcam$^{+/-}$Arg-1^{lo}Gal-3^{lo}Col-VI^{lo}	45	335	Col-VI+ cytotoxic neutrophils
3	CD45$^{+/-}$Epcam^{+}CD11c^{+}Gal-3^{hi}Arg-1^{lo}Col-VI^{lo}	105	210	Dendritic cells
4	Epcam^{+}Gal-3^{+}Arg-1^{lo}K14^{lo}CD11b^{lo}	10	302	Gal-3+ tumor
5	CD31+Epcam+/-Col-IV+Col-VI+/-	82	219	Col-VI+Col-IV+Epcam+ endothelium
6	Epcam^{+}Col-VI^{+}Arg-1^{lo}	116	175	Col-VI+ tumor
7	Epcam^{+}MMP2^{+}	33	257	MMP2+ tumor
8	MMP2^{+}Col-VI^{+}	15	265	Col-VI+ MMP2+
9	Epcam^{+}K14^{hi}Col-VI^{lo}Gal-3^{lo}	0	279	Col-VI invasive tumor
10	Col-VI^{+}Gal-3$^{+/-}$K14^{lo}Arg-1^{lo}	14	244	Col-VI
11	Epcam^{+}SOX9^{+}Arg-1^{lo}K14^{hi}Gal-3^{lo}	55	201	Arg-1+K14+ cancer stem cells
12	CD45^{+}Epcam^{+}Arg-1^{+}	224	19	Arg-1+ Epcam+ leukocytes
13	Epcam^{hi}CD45$^{+/-}$CD11b^{lo}Col-VI^{+}Fal-3^{hi}Arg-1^{lo}MPO^{lo}	51	173	Col-VI+ Epcam+ leukocytes
14	Epcam^{+}Ki67^{+}	19	205	Proliferating tumor
15	Epcam^{+}SOX9^{+}	2	216	Cancer stem cells
16	Epcam^{+}Cd45^{hi}F480^{+}Gal-3^{lo}Arg-1^{lo}	60	142	Macrophages
17	Epcam^{+}Col-VI^{+}	60	125	Col-VI+ tumor
18	Epcam^{hi}CD31^{hi}Col-VI^{hi}MMP2^{hi}	53	130	Col-VI+MMP2+Epcam+ endothelium
19	Epcam+Arg-1+Ki67+	146	29	Arg-1+ proliferating tumor
20	Epcam^{+}CD45$^{+/-}$CD11c^{+}F480^{hi}SOX9$^{+/-}$Col-VI^{lo}Arg-1^{lo}CD11b^{lo}Gal-3^{lo}Col-IV^{lo}	22	151	F480+ dendritic cells
21	Epca,$^{+/-}$CD45^{hi}CD11b^{lo}CSF1R^{+}F480^{lo}MPO^{lo}Gal-3^{lo}CD11c^{lo}CC3^{lo}	19	133	CSF1R+ macrophages
22	Col-VI^{+}	12	135	Col-VI
23	Epcam^{+}K14^{+}	1	125	Invasive tumor
24	MMP2^{+}	15	107	MMP2
25	Epcam^{+}Arg-1^{+}MMP2^{+}	111	11	MMP2+ Arg-1+ tumor
26	Epcam^{+}CD45^{hi}CD31^{lo}Gal-3^{lo}	29	88	Epcam+ leukocytes
27	Col-VI^{+}	7	98	Col-VI
28	aSMA^{+}Epcam^{hi}Col-VI^{hi}SOX9^{lo}CD11c^{lo}CD31^{lo}F480^{lo}Col-IV^{lo}Gal-3^{lo}Ki67^{lo}CD11b^{lo}CD45^{lo}	0	101	Mesenchymal cells/EMT
29	Epcam^{+}CD31^{+}Arg-1^{+}Col-IV^{+}	96	1	Col-IV+ Arg-1+ endothelium
30	CD31^{+}Epcam$^{+/-}$Col-IV^{+}MMP2^{+}Col-VI^{hi}	12	79	Col-VI+Col-IV+MMP2+ endothelium
31	SOX9^{+}K14^{lo}	0	51	Cancer stem cells
32	Epcam^{hi}MMP2^{+}Col-IV^{+}Col-VI^{hi}Arg-1^{lo}	14	37	MMP2+ Col-IV+ Col-VI+ tumor
33	Arg-1^{+}	31	11	Arg-1
34	Epcam^{+}CD31^{+}Arg-1^{+}	31	2	Epcam+ Arg-1+ endothelium
Replicate 2		Ratio		
Cluster	Marker combination	ctrl	pano	Phenotype
0	Epcam^{+}Ki67^{+}	616	154	Proliferating tumor
1	Epcam^{+}Ki67^{+}	203	382	Proliferating tumor
2	Epcam^{+}Ki67^{+}	403	116	Proliferating tumor
3	MMP2^{+}Col-VI^{+}	3	404	Col-VI+ MMP2+
4	Epcam^{+}Col-VI^{+}	93	312	Col-VI+ tumor
5	CD45^{hi}CD11b^{hi}MPO^{hi}Col-VI^{hi}Epcam$^{+/-}$MMP2^{lo}Col-IV^{lo}	12	379	Col-VI+ cytotoxic neutrophils
6	CD45$^{+/-}$ Epcam$^{+/-}$Gal-3^{hi}Col-VI$^{+/-}$Ki67^{lo}	105	234	Gal-3+Epcam+Col-VI+ leukocytes
7	Epcam^{hi}CD45^{hi}CD11c^{+}CD11b^{-}Gal-3^{lo}Col-VI^{lo}MMP2^{lo}Col-IV^{lo}Ki67^{lo}	232	103	Dendritic cells
8	Epcam^{+}Arg-1^{+}Gal-3^{lo}MPO^{lo}CD11b^{lo}Col-VI^{lo}CD45^{lo}	46	266	Arg-1+ tumor
9	Epcam^{+}CD31^{+}Col-VI^{hi}Col-IV^{+}MMP2^{lo}Ki67^{lo}	234	51	Col-VI+Col-IV+Epcam+ endothelium
10	Epcam^{+}Col-VI^{+}MMP2^{+}	5	278	Col-VI+ MMP2+ tumor
11	Epcam^{+}K14^{+}	7	272	Invasive tumor
12	Epcam$^{+/-}$K14^{hi}Col-VI^{hi}MMP2^{lo}	1	270	Col-VI+MMP2+ Invasive tumor
13	Epcam^{hi}CD45$^{+/-}$F480^{+}CD11c^{hi}CD11b^{lo}Gal-3^{hi}Col-VI^{lo}MMP2^{lo}Col-IV^{lo}Arg-1^{lo}	38	198	F480+ dendritic cells
14	CD31^{hi}Col-VI^{hi}MMP2^{+}Col-IV^{+}	8	211	Col-VI+Col-IV+MMP2+ endothelium
15	Epcam^{hi}Col-VI^{hi}Col-IV^{+}	97	106	Col-VI+Col-IV+ tumor
16	Epcam^{+}MMP2^{+}	0	199	MMP2+ tumor
17	aSMA^{+}Epcam^{hi}Col-VI^{hi}Col-IV^{hi}MMP2^{lo}Gal-3^{lo}CD45^{loCD31lo}	52	133	Mesenchymal cells/EMT
18	Ki67^{+}	4	179	Proliferation
19	Epcam^{+}CD45^{+}	172	10	Epcam+ leukocytes
20	Epcam^{hi}SOX9^{+}aSMA^{lo}Col-VI^{lo}Arg-1^{lo}CD11b^{lo}Ki67^{lo}F480^{lo}Col-IV^{lo}CD11c^{lo}CD31^{lo}	5	176	Cancer stem cells
21	CD31$^{+/-}$Col-VI^{hi}Col-IV$^{+/-}$	19	160	Col-VI+Col-IV+ endothelium
22	Epcam^{+}Col-IV^{+}	153	25	Col-IV+ tumor
23		56	122	background
24	Epcam^{+}Gal-3^{+}	44	115	Gal-3+ tumor
25	Epcam^{+}K14$^{+/-}$Ki67$^{+/-}$Col-VI^{lo}	18	126	Proliferating invasive tumor
26	Col-VI^{+}	20	105	Col-VI
27	Epcam$^{+/-}$Ki67$^{+/-}$MMP2^{+}	5	117	MMP2+ proliferating tumor
28	Epcam^{+}CC3^{+}CD11c^{lo}CD31^{lo}CD45^{lo}CD11b^{lo}Ki67^{lo}MPO^{lo}Col-VI^{lo}F480^{lo}MMP2^{lo}Col-IV^{lo}	29	79	Dying tumor
29	Epcam^{+}CD45^{+}Col-VI^{hi}Col-IV^{+}CD11b^{lo}	33	61	Col-VI+Col-IV+Epcam+ leukocytes
30	K14^{+}	0	90	Invasion
31	Epcam^{+}Ki67^{+}Col-IV^{+}Col-VI^{lo}	73	15	Col-IV+ proliferating tumor
32	K14^{hi}MMP2^{+}Col-IV^{hi}Col-VI$^{+/-}$	1	75	MMP2+Col-IV+Col-VI+ invasive tumor
33	Col-VI^{+}	3	62	Col-VI
34	Epcam^{+}CD45^{+}CSF1R^{+}CD11c^{+}Gal-3^{lo}Ki67^{lo}	53	4	CSF1R+ DC
35	Ki67^{+}Col-VI^{+}	1	12	Ki67^{+}Col-VI^{+}
36	Epcam^{+}Ki67^{+}Col-VI^{+}MMP2^{+}	0	11	MMP2+Col-VI+ proliferating tumor

Supplementary Table 2 | Cluster marker combinations for 4 replicates. The table states each cluster, the proportion of control and panobinostat cells and the annotation.

Replicate 3				
Cluster	Marker combination	ctrl	pano	Phenotype
0	Epcam^{+}Ki67^{+}	218	292	Proliferating tumor
1	Epcam^{+}Col-VI^{+}	203	252	Col-VI tumor
2	Epcam^{+}Ki67^{+}	167	201	Proliferating tumor
3	CD31^{+}Col-VI^{+}Col-IV^{+}MMP2$^{+/-}$	158	177	Col-VI+Col-IV+MMP2+ endothelium
4	MMP2^{+}Col-VI^{+}	57	276	Col-VI+ MMP2+
5	Epcam^{hi}K14^{+}Col-VI^{lo}	23	275	Col-VI+ invasive tumor
6	Epcam^{+}K14^{+}	7	266	Invasive tumor
7	CD45^{hi}CD11c^{+}Col-VI^{lo}	167	101	Dendritic cells
8	Epcam^{+}CD45^{+}	231	24	Epcam+ leukocytes
9	CD45^{+}CD11b^{+}MPO^{hi}Epcam$^{+/-}$Col-VI^{hi}MMP2^{lo}Col-IV^{lo}	10	242	Col-VI+ cytotoxic neutrophils
10	Epcam^{+}Arg-1^{+}Gal-3^{hi}Col-VI^{lo}Col-IV^{lo}	0	247	Arg-1+Gal-3+ tumor
11	Epcam^{+}Col-VI^{+}MMP2^{+}	72	154	Col-VI+ MMP2+ tumor
12	CD45^{+}Epcam$^{+/-}$Col-VI$^{+/-}$Ki67^{lo}	158	62	Col-VI+Epcam+ leukocytes
13	Epcam^{+}SOX9^{+}Col-VI^{lo}CD31^{lo}Col-IV^{lo}MMP2^{lo}CC3^{lo}	25	182	Cancer stem cells
14	Epcam^{+}MMP2^{+}	29	173	MMP2+ tumor
15	Col-VI^{+}	92	77	Col-VI
16	Epcam^{+}Gal-3^{hi}Col-VI$^{+/-}$Col-IV^{lo}MMP2^{lo}CD11c^{lo}	5	159	Gal-3+Col-VI+ tumor
17	aSMA^{+}Epcam^{hi}SOX9^{hi}CD31^{hi}Col-IV^{hi}Col-VI^{hi}CC3$^{+/-}$Ki67^{lo}F480^{lo}Gal-3^{lo}	39	124	Mesenchymal cells/EMT
18	Epcam^{+}Ki67^{+}	36	125	Proliferating tumor
19	Epcam^{hi}CD45^{hi}F480^{+}Col-VI^{lo}MMP2^{lo}Col-IV^{lo}	61	92	Macrophages
20	Epcam^{+}CD45^{hi}CD11c^{+}F480^{+}SOX9^{lo}	74	77	F480+ dendritic cells
21	Epcam^{+}Col-VI^{+}	92	55	Col-VI tumor
22	Epcam^{+}CC3^{+}F480^{lo}	49	93	Dying tumor
23	CD31^{hi}Epcam^{+}Col-IV^{+}Col-VI^{hi}	75	66	Col-VI+Col-IV+Epcam+ endothelium
24	CD31^{hi}Epcam^{lo}Col-VI^{hi}Ki67^{lo}	58	63	Col-VI+ endothelium
25	Col-VI^{+}	50	60	Col-VI
26	CD45^{hi}Epcam^{hi}MPO^{+}Col-VI^{lo}	6	93	Col-VI+ cytotoxic neutrophils
27	Ki67^{+}	51	45	Proliferation
28	CD45^{hi}Epcam$^{+/-}$CSF1R^{+}F480$^{+/-}$CD11c^{lo}CD11b^{lo}MPO^{lo}Col-VI^{lo}MMP2^{lo}	60	35	CSF1R+ macrophages
29	CD45^{lo}MMP2^{+}Col-VI^{lo}	32	60	MMP2+ leukocytes
30	Ki67^{+}	38	48	Proliferation
31	Col-VI^{+}	31	42	Col-VI
32	Col-VI+Col-IV+	35	27	Col-VI+Col-IV+
33	CD31^{+}MMP2^{+}Col-VI^{hi}Epcam^{lo}	4	56	Col-VI+MMP2+ endothelium
34	Col-VI+MMP2+Col-IV+	10	23	Col-VI+ MMP2+
35	SOX9+	2	17	Cancer stem cells
36	SOX9^{+}Epcam^{+}Arg-1^{+}K14$^{+/-}$	0	18	Arg-1+K14+ cancer stem cells
Replicate 4				
Cluster	Marker combination	ctrl	pano	Phenotype
0	Epcam^{+}MMP2^{+}	367	176	MMP2+ tumor
1	Epcam^{+}Col-VI^{+}	46	478	Col-VI+ tumor
2	Epcam^{+}Gal-3^{+}Arg-1^{+}CD11c^{lo}	24	384	Arg-1+Gal-3+ tumor
3	Epcam^{+}Col-VI^{+}MMP2^{+}	179	190	Col-VI+MMP2+ tumor
4	Epcam^{+}CD45^{hi}CD11c^{+}Col-VI^{lo}MMP2^{lo}	252	95	Dendritic cells
5	Epcam^{+}K14^{+}	38	304	Invasive tumor
6	Epcam^{+}MMP2^{+}	329	0	MMP2+ tumor
7	Epcam^{+}SOX9^{+}	14	299	Cancer stem cells
8	Epcam^{+}CD45^{hi}F480^{+}CD11c^{hi}MMP2^{lo}Col-VI^{lo}Col-IV^{lo}	250	50	F480+ dendritic cells
9	Epcam^{+}Col-VI^{+}	6	284	Col-VI+ tumor
10	Epcam^{+}CD45^{+}MMP2^{lo}	230	44	Epcam+ leukocytes
11	Epcam^{+}CD45^{+}CD11b^{+}MMP2$^{+/-}$Col-VI^{lo}Col-IV^{lo}	203	51	Epcam+ myeloid cells
12	Epcam^{+}MMP2^{+}	245	7	MMP2+ tumor
13	Epcam^{+}CD45^{hi}CD11b^{hi}MPO^{+}Col-VI^{lo}MMP2^{lo}	167	81	Cytotoxic neutrophils
14	Epcam^{+}Col-IV^{+}	71	168	Col-IV+ tumor
15	Epcam^{+}aSMA^{+}Col-VI^{lo}MMP2^{lo}	3	235	EMT
16	Epcam^{+}Ki67^{+}	81	110	Proliferating tumor
17	aSMA^{+}Col-VI$^{+/-}$MMP2^{lo}	0	190	Col-VI+ mesenchymal cells
18	Epcam^{+}CD31^{+}Col-IV^{+}	87	86	Col-IV+Epcam+ endothelium
19	Epcam^{+}K14^{+}Col-VI^{hi}Col-IV^{lo}MMP2^{lo}	25	140	Col-VI+ invasive tumor
20	Epcam^{+}CD31^{+}Col-IV^{+}MMP2^{+}Col-VI^{lo}	123	39	Col-IV+MMP2+Epcam+ endothelium
21	Col-VI^{+}	6	153	Col-VI
22	Epcam^{+}CC3^{+}CD45^{lo}CD22b^{lo}Ki67^{lo}Gal-3^{lo}MPO^{lo}F480^{lo}MMP2^{lo}Col-IV^{lo}Arg-1^{lo}	28	113	Dying tumor
23	CD31^{hi}Col-IV^{+}Col-VI^{lo}	2	129	Col-VI+Col-IV+ endothelium
24	Epcam^{+}SOX9^{+}K14^{lo}Col-VI^{lo}Col-IV^{lo}MMP2^{lo}	8	116	K14+ stem cells
25	Epcam^{+}CD31^{+}MMP2$^{+/-}$	91	15	MMP2+ endothelium
26	CD45^{+}CD11b^{+}MPO^{hi}CSF1R^{+}CD11c^{lo}MMP2^{lo}	101	3	CSF1R+ myeloid cells
27	Epcam^{+}aSMA^{+}Col-VI^{+}	0	85	Col-VI+ EMT
28	Epcam^{+}Col-VI^{+}Col-IV^{+}	1	82	Col-VI+Col-IV+ tumor
29	Col-VI^{+}MMP2^{+}	11	63	Col-VI+ MMP2+
30	K14^{+}Col-IV^{lo}	0	65	Invasion
31	Epcam^{+}CD31^{+}Col-VI^{+}Col-IV^{+}	8	49	Col-VI+Col-IV+Epcam+ endothelium
32	Epcam^{+}Arg-1^{+}CD45^{lo}Col-VI^{lo}	0	44	Arg-1+ tumor
33	MMP2^{+}	0	27	MMP2
34	Ki67^{+}Col-VI^{lo}	0	8	Ki67+Col-VI+

Supplementary Table 2 | Cluster marker combinations for 4 replicates. The table states each cluster, the proportion of control and panobinostat cells and the annotation (continued).

	d0	d3	d7	d10	d17	d21	d24
Control + IgG2a	386.89	683.79	951.27	1318.23	1895.34	2468.8	3026.18
	364.84	623.71	987.13	1464.18	1967.21	2491.01	3200.07
	406.96	693.34	1264.64	1690.72	2125.67	2446.18	2864.1
	210.65	327.21	788.66	1109.94	1657.05	2220.18	2624.11
	207.12	499.91	777.13	1144.87	1546.11	1926.2	2362.33
	261.07	404.42	603.31	1029.68	1648.28	2253.3	2753.73
	177.34	284.97	424.54	753.1	1331.32	1866.53	2398.58
	208.58	353.69	580.65	915.67	1576.44	2098.4	2563.43
Pano + IgG2a	399.91	726.61	913.99	1389.1	1602.96	2065.22	2490.89
	350.02	689.89	1200.97	1523.79	1983.65	2425.44	2944.83
	210.08	315.36	576.68	818.48	1043.12	1323.14	1861.67
	189.87	267.04	431.08	532.52	808.69	1010.44	1587.52
	413.63	680.65	1206.05	1766.76	2129.06	2488.21	3079.67
	217.93	353.58	708.3	1197.24	1745.48	1981.95	2476.16
	325.24	500.59	796.18	1103.07	1390.46	1826.17	2598.1
	200.29	336.81	418.04	734.04	1176.95	1465.55	1875.03
Pano + aPD1	397.21	745.81	1030.2	1355.68	1525.06	1846.93	2223.16
	263.14	405.13	601.55	809.2	967.43	1119.41	1541.51
	512.55	710.3	1172.5	1317.66	1457.96	1790.12	2262.63
	205.68	255.12	465.18	522.36	604.96	783.93	1084.42
	134.78	237.17	338.43	578.52	805.57	1052.94	1462.85
	228.66	360	508.84	699.98	993.45	1354.11	1867.61
	290.28	439.76	625.43	835.9	944.4	1397.19	1875.29
	184.67	358.6	522.01	658.41	884.24	1216.49	1613.29
Pano + Los	319.04	543.12	684.12	901.86	1074.07	1287.89	1550.23
	387.13	701.27	937.71	1135.87	1335.35	1722.36	2175.65
	167.21	232.91	313.51	478.65	663.62	763.44	1090.94
	471.83	585.43	938.56	1083.84	1385.88	1549.21	1840.22
	412.57	601.27	754.28	871.39	1190.24	1523.89	2080.7
	193.5	434.45	626.73	829.68	1142.55	1514.63	1936.79
	241.93	316.76	413.15	630.3	1082.08	1372.56	1743.33
	190.9	306.55	497.14	663.28	1179.17	1598.02	2086.2
Pano + aPD1 + Los	320.83	436.1	537.58	609.73	793.16	935.42	1216.78
	440.58	610.71	731.88	804.54	895.19	973.12	1208.83
	179.38	290.16	367.39	471.92	526.23	702.97	882.07
	287.89	559.93	789.99	902.46	1186.66	1338.17	1679.31
	211.88	390.47	525.2	615.42	915.57	1147.54	1357.41
	209.93	315.01	362.22	410.35	562.49	676.27	931.25
	190.36	272.23	321.87	401.01	555.48	665.75	755.04
	237.88	348.53	430.61	508.17	665.55	761.73	878.19

Supplementary Table 3 | Tumor measurement source data for Fig. 6C. Tumor measurements of 8 mice per systemic treatment group. Volume is given in mm^3 and endpoint was defined as one measurement above 2500 mm^3. Pano, panobinostat; Los, Losartan.